Available online at www.sciencedirect.com

ScienceDirect

Procedia Engineering 199 (2017) 2140–2145

Procedia Engineering

www.elsevier.com/locate/procedia

X International Conference on Structural Dynamics, EURODYN 2017

On the use of equivalent forces for structural health monitoring based on joint input-state estimation algorithms

E. Lourens[a,*], D.J.M. Fallais[a]

[a] *Faculty of Civil Engineering and Geo Science, Delft University of Technology, Stevinweg 1, 2628 CN Delft, The Netherlands*

Abstract

For the monitoring of large structures where the loading is typically characterized by large uncertainties in temporal and/or spatial evolution, algorithms capable of estimating a set of response driving equivalent forces are strongly desired. In this context, several Kalman-type coupled input-state and coupled input-state-parameter filters have recently been developed, allowing for an estimation of the full-field dynamic response of a structure from only a limited number of vibration measurements. Up to now, the success of response estimation based on the identification of equivalent forces has been related only to whether these forces satisfy the so-called controllability requirements. In this contribution, controllability is shown to be an insufficient criterion for guaranteeing the accuracy of response estimates based on equivalent loading. Instead, the need for a new criterion is advocated, which would allow to assess the applicability of equivalent force based monitoring to various engineering problems. Concepts are illustrated by comparing true and assumed noise statistics as well as the response prediction accuracy for different numerical examples, where a) the applied and equivalent loads are concentrated and collocated, b) the applied and equivalent loads are concentrated and non-collocated, and c) modal equivalent forces are used. Results are applicable to any Kalman-type coupled input-state estimator derived using the principles of minimum-variance unbiased estimation.

Peer-review under responsibility of the organizing committee of EURODYN 2017.

Keywords: Kalman filter, equivalent forces, controllability, response prediction, structural health monitoring.

1. Introduction

Commonly employed vibration sensors, e.g. accelerometers and strain gauges, provide only local information on the dynamic response of a structure. In many situations, however, knowledge of the full-field structural response is required. Consider for instance the monitoring of accumulated fatigue damage at critical locations that are inaccessible for measurements, e.g. the location just below the seabed on an offshore wind turbine foundation [1,2]. Monitoring of the full-field response of a structure in conjunction with the forces applied to it can also be used to obtain insights into complex interaction phenomena, e.g. ice-induced vibrations [3,4]. In recent years, a number of inverse methodologies for the extrapolation of structural response to unmeasured locations have been proposed. In this contribution, we consider only the Kalman-type filters, where modelling as well as measurement errors are included in the estimation

* Corresponding author. Tel.: +31 (0)15 27 88030.
E-mail address: E.Lourens@tudelft.nl

1877-7058
Peer-review under responsibility of the organizing committee of EURODYN 2017.
10.1016/j.proeng.2017.09.152

process as stochastic processes of which only the variances are known. These techniques can be divided into filters that rely on some assumptions regarding the type of loading (e.g. white noise) [5], and filters that observe full-field structural response in the absence of any knowledge of the dynamic evolution of the applied loading [6]. We will focus on the latter, and more specifically on cases in which also the spatial distribution of the loading is assumed unknown, and a set of response-driving equivalent forces is identified from the measurements. Through careful analysis of the assumptions forming the basis for the derivation of these algorithms and their possible violation in various real-life applications, the limitations of response estimation based on equivalent loading is exemplified. The presented situations include those in which the locations of the forces are only known approximately, and those in which modal equivalent forces are assumed.

2. Coupled state and input estimation

Consider the equations of motion for a linear structural system discretized in space as presented in Eq. (1):

$$\mathbf{M}\ddot{\mathbf{u}}(t) + \mathbf{C}\dot{\mathbf{u}}(t) + \mathbf{K}\mathbf{u}(t) = \mathbf{f}(t) = \mathbf{S}_\mathrm{p}(t)\mathbf{p}(t) \tag{1}$$

$$\dot{\mathbf{x}}(t) = \mathbf{A}_\mathrm{c}\mathbf{x}(t) + \mathbf{B}_\mathrm{c}\mathbf{p}(t) \tag{2}$$

$$\mathbf{d}(t) = \mathbf{G}_\mathrm{c}\mathbf{x}(t) + \mathbf{J}_\mathrm{c}\mathbf{p}(t) \tag{3}$$

where $\mathbf{M}$, $\mathbf{C}$ and $\mathbf{K} \in \mathbb{R}^{n_\mathrm{dof}\times n_\mathrm{dof}}$ denote the mass, damping and stiffness matrix, respectively, and $\mathbf{f}(t)$ is the excitation vector. In what follows it is assumed that the response of the system can be accurately described by means of a limited number of n_m modes, as $\mathbf{u}(t) = \mathbf{\Phi}\mathbf{z}(t)$ with $\mathbf{\Phi} \in \mathbb{R}^{n_\mathrm{dof}\times n_m}$ and $n_m < n_\mathrm{dof}$. By defining a modal state vector, $\mathbf{x}(t) = \{\mathbf{z}(t)\ \dot{\mathbf{z}}(t)\}^\mathrm{T} \in \mathbb{R}^{n_\mathrm{s}}$, Eq. (1) can be transformed to first-order state-space form, as shown in Eq. (2) and (3), where $\mathbf{x}(\mathrm{t}) \in \mathbb{R}^n$, and:

$$\mathbf{A}_\mathrm{c} = \begin{bmatrix} \mathbf{0} & \mathbf{I} \\ -\mathbf{\Omega}^2 & -\mathbf{\Gamma} \end{bmatrix}, \quad \mathbf{B}_\mathrm{c} = \begin{bmatrix} \mathbf{0} \\ \mathbf{\Phi}^\mathrm{T}\mathbf{S}_\mathrm{p} \end{bmatrix}, \quad \mathbf{G}_\mathrm{c} = \begin{bmatrix} \mathbf{S}_\mathrm{d}\mathbf{\Phi} - \mathbf{S}_\mathrm{a}\mathbf{\Phi}\mathbf{\Omega}^2 & \mathbf{S}_\mathrm{v}\mathbf{\Phi} - \mathbf{S}_\mathrm{a}\mathbf{\Phi}\mathbf{\Gamma} \end{bmatrix}, \quad \mathbf{J}_\mathrm{c} = \begin{bmatrix} \mathbf{S}_\mathrm{a}\mathbf{\Phi}\mathbf{\Phi}^\mathrm{T}\mathbf{S}_\mathrm{p} \end{bmatrix}. \tag{4}$$

The matrices $\mathbf{\Omega}^2$ and $\mathbf{\Gamma}$ are defined as $\mathbf{\Omega}^2 = \mathbf{\Phi}^\mathrm{T}\mathbf{K}\mathbf{\Phi} = \mathrm{diag}(\omega_j^2)$ and $\mathbf{\Gamma} = \mathrm{diag}(2\xi_j\omega_j^2)$. Discretization of Eq. (2) and (3) assuming constant intersample behaviour of the inputs, and the addition of the stochastic noise processes $\{\mathbf{w}_k\}_{k=1}^\infty$ and $\{\mathbf{v}_k\}_{k=1}^\infty$ representing respectively process and measurement errors, leads to Eq. (5) and (6), with $\mathbf{A}, \mathbf{B}, \mathbf{G}, \mathbf{J}$ defined in Eq. (7).

$$\mathbf{x}_{k+1} = \mathbf{A}\mathbf{x}_k + \mathbf{B}\mathbf{p}_k + \boldsymbol{w}_k \tag{5}$$

$$\mathbf{d}_k = \mathbf{G}\mathbf{x}_k + \mathbf{J}\mathbf{p}_k + \boldsymbol{v}_k. \tag{6}$$

$$\mathbf{A} = e^{\mathbf{A}_\mathrm{c}\Delta t},\ \mathbf{B} = [\mathbf{A} - \mathbf{I}]\mathbf{A}_\mathrm{c}^{-1}\mathbf{B}_\mathrm{c},\ \mathbf{G} = \mathbf{G}_\mathrm{c},\ \mathbf{J} = \mathbf{J}_\mathrm{c} \tag{7}$$

A number of Kalman-type filters have recently been proposed for jointly estimating the states $\mathbf{x}$ and input $\mathbf{p}$ on the basis of a set of measurements $\mathbf{d}$ and the system of equations presented above. Due to space limitations these algorithms will not be presented; instead we refer to [7] for a recent comparison. The results presented in the following sections were all generated with the joint input-state estimator [8], but the conclusions are valid for any Kalman-type coupled input-state estimator derived using the principles of minimum-variance unbiased estimation.

3. Noise process assumptions

The noise processes are in general characterized as zero-mean, white noise signals with known covariance matrices:

$$\mathbb{E}[\boldsymbol{w}_k] = \mathbb{E}[\boldsymbol{v}_k] = 0 \tag{8}$$

$$\mathbb{E}\left\{ \begin{bmatrix} \boldsymbol{w}_k \\ \boldsymbol{v}_k \end{bmatrix} \begin{bmatrix} \boldsymbol{w}_l^\mathrm{T} & \boldsymbol{v}_l^\mathrm{T} \end{bmatrix} \right\} = \begin{bmatrix} \mathbf{Q} & \mathbf{S} \\ \mathbf{S} & \mathbf{R} \end{bmatrix} \delta_{kl}. \tag{9}$$

In the remainder of the paper, the focus will be on the effect of having discrepancies between the theoretical assumptions above and the physical situation, especially focusing on the consequences hereof with regard to the uniqueness of the estimates.

4. Response prediction using equivalent forces

The state and force estimates - $\hat{\mathbf{x}}$ and $\hat{\mathbf{p}}$ - obtained with the filters can be used to estimate the full-field response of a structure on the basis of limited sensor data. The idea was first presented in [6], and involves reformulating a new observation equation as follows:

$$\hat{\mathbf{d}}_{\mathrm{ex},k} = \mathbf{G}_{\mathrm{ex}}\hat{\mathbf{x}}_k + \mathbf{J}_{\mathrm{ex}}\hat{\mathbf{p}}_k \tag{10}$$

where $\hat{\square}$ denotes an estimated quantity, and the subscript $\square_{\mathrm{ex}}$ abbreviates extrapolated. When a set of equivalent forces $\hat{\mathbf{p}}$ is identified, the process and measurement noise $\boldsymbol{w}_k$ and $\boldsymbol{v}_k$ in Eq. (5) and (6) can be divided into contributions from force location errors, modelling errors, and sensor noise. For reduced-order systems constructed using Eq. (4) or (7), modelling errors consist of specifically eigenfrequency, eigenmode, and damping errors, i.e. errors on the dynamic properties. One can write Eq. (11) and (12):

$$\boldsymbol{w}_k = \{\boldsymbol{w}_k\}_{\mathrm{force}} + \{\boldsymbol{w}_k\}_{\mathrm{prop}} \tag{11}$$

$$\boldsymbol{v}_k = \{\boldsymbol{v}_k\}_{\mathrm{force}} + \{\boldsymbol{v}_k\}_{\mathrm{prop}} + \{\boldsymbol{v}_k\}_{\mathrm{sensor}} \tag{12}$$

$$\{\boldsymbol{w}_k\}_{\mathrm{force}} = \mathbf{B}_{\mathrm{real}}\mathbf{p}_{k,\mathrm{real}} - \mathbf{B}_{\mathrm{eq}}\hat{\mathbf{p}}_k \tag{13}$$

$$\{\boldsymbol{v}_k\}_{\mathrm{force}} = \mathbf{J}_{\mathrm{real}}\mathbf{p}_{k,\mathrm{real}} - \mathbf{J}_{\mathrm{eq}}\hat{\mathbf{p}}_k \tag{14}$$

Defining $\square_{\mathrm{real}}$ and $\square_{\mathrm{eq}}$ as the matrices/vectors corresponding to respectively the real and equivalent force locations, the contributions from errors on these locations can be further specified as presented in Eq. (13) and (14), where $\mathbf{B}_{\mathrm{eq}}$ and $\mathbf{J}_{\mathrm{eq}}$ are constructed according to Eq. (4) using the assumed locations of the equivalent forces. Note that the two stochastic error processes become correlated – $\mathbf{S} = \mathbb{E}\{\boldsymbol{w}_k\boldsymbol{v}_k^{\mathrm{T}}\} \neq \mathbf{0}$; cf. Eq. (9) – and are possibly no longer white.

Recalling again that $\mathbf{Q} = \mathbb{E}\{\boldsymbol{w}_k\boldsymbol{w}_l^{\mathrm{T}}\}$ and $\mathbf{R} = \mathbb{E}\{\boldsymbol{v}_k\boldsymbol{v}_l^{\mathrm{T}}\}$, an additional distinction is made between real and assumed covariances:

$$\mathbf{Q}_{\mathrm{e}} = \mathbf{Q}_{\mathrm{real}} - \mathbf{Q}_{\mathrm{as}}, \quad \mathbf{R}_{\mathrm{e}} = \mathbf{R}_{\mathrm{real}} - \mathbf{R}_{\mathrm{as}}, \quad \mathbf{S}_{\mathrm{e}} = \mathbf{S}_{\mathrm{real}} - \mathbf{S}_{\mathrm{as}} \tag{15}$$

where the subscripts ‘e’ and ‘as’ denote error and assumed, respectively, and the real covariances are those specified in equations (11) and (12). These matrices can be further decomposed into blocks representing the (co)variances between the modal displacements $\mathbf{z}$, the modal velocities $\dot{\mathbf{z}}$, and the data $\mathbf{d}$, respectively:

$$\mathbf{Q}_{\mathrm{e}} = \begin{bmatrix} \mathbf{Q}_{\mathrm{e},\mathbf{zz}} & \mathbf{Q}_{\mathrm{e},\mathbf{z\dot{z}}} \\ \mathbf{Q}_{\mathrm{e},\dot{\mathbf{z}}\mathbf{z}} & \mathbf{Q}_{\mathrm{e},\dot{\mathbf{z}}\dot{\mathbf{z}}} \end{bmatrix}, \quad \mathbf{S}_{\mathrm{e}} = \begin{bmatrix} \mathbf{S}_{\mathrm{e},\mathbf{zd}} \\ \mathbf{S}_{\mathrm{e},\dot{\mathbf{z}}\mathbf{d}} \end{bmatrix} \tag{16}$$

where, $\mathbf{Q}_{\mathrm{e},\mathbf{zz}}$, $\mathbf{Q}_{\mathrm{e},\mathbf{z\dot{z}}}$, $\mathbf{Q}_{\mathrm{e},\dot{\mathbf{z}}\dot{\mathbf{z}}} \in \mathbb{R}^{(\mathrm{n_s}/2)\times(\mathrm{n_s}/2)}$ and $\mathbf{S}_{\mathrm{e},\mathbf{zd}}$, $\mathbf{S}_{\mathrm{e},\dot{\mathbf{z}}\mathbf{d}} \in \mathbb{R}^{(\mathrm{n_s}/2)\times \mathrm{n_d}}$.

5. Numerical examples

A 21-node cantilever beam model is constructed based on Euler-Bernoulli beam theory and consequently reduced to 10 DOFs on the basis of the first 10 modes. The properties of the beam are as follows: length $L = 1$m, mass $m = 1$kg, and bending stiffness $EI = 1$ Nm^2. Modal damping of $\xi = 2\%$ is assumed for all modes. The first three natural frequencies of the beam are 0.56, 3.51, and 9.82 Hz, respectively. The excitation is chosen as a superposition of two harmonic forces with frequencies equal to 2.03 Hz and 6.66 Hz, and is applied at the tip of the beam. These frequencies are chosen as the average of respectively the first and second, and second and third natural frequency of the structure. A sampling frequency of 1000 Hz is used in all the following examples, satisfying the Nyquist-Shannon sampling criterion with respect to the highest load frequency and all structural frequencies up to the 6$^{\mathrm{th}}$ mode. It is mentioned that when the coupled input-state estimation is performed based on real data, the selected time step size should also be chosen with regard to the physical delay in the system, in order to ensure that causality is respected [9,10]. Simulated measurement data from 4 accelerometers and 1 strain gauge is used for the estimation. Accelerations are simulated at: $L/4$, $L/2$, $3L/4$ and L whereas the strain is simulated at $L/4$. Unless states otherwise, the chosen data set and (equivalent) force locations satisfy the observability and direct invertibility criteria as formulated in [11] for all cases analyzed. To rule out potential initialization or convergence effects the first 10 seconds are neglected during the post processing. To analyze the effect of equivalent force assumptions, no structural modelling errors will be considered,

implying that the error processes in Eq. (11) and (12) reduce to $\{\boldsymbol{w}_k\} = \{\boldsymbol{w}_k\}_{\text{force}}$ and $\{\boldsymbol{v}_k\} = \{\boldsymbol{v}_k\}_{\text{force}} + \{\boldsymbol{v}_k\}_{\text{sensor}}$. In order to minimize the effect of measurement noise, the standard deviation of the noise added to each simulated measurement is assumed equal to the standard deviation of the measurement multiplied by a factor $1e^{-6}$. The assumed noise matrix $\mathbf{R}_{\text{as}}$ is constructed so as to be consistent with the added sensor noise, so that $\mathbf{R}_{\text{e}}$ of Eq. (15) is related solely to the force positions: $\mathbf{R}_{\text{e}} = \mathbb{E}\left[\{\boldsymbol{v}_k\}_{\text{force}}\{\boldsymbol{v}_k\}_{\text{force}}^T\right]$. By also assuming $\mathbf{Q}_{\text{as}} = 0$ and $\mathbf{S}_{\text{as}} = 0$ in all of the presented analyses, $\mathbf{Q}_{\mathbf{e}}$ and $\mathbf{S}_{\mathbf{e}}$ can be similarly related solely to an error on the force positions: $\mathbf{Q}_{\text{e}} = \mathbb{E}\left[\{\boldsymbol{w}_k\}_{\text{force}}\{\boldsymbol{w}_k\}_{\text{force}}^T\right]$ and $\mathbf{S}_{\text{e}} = \mathbb{E}\left[\{\boldsymbol{w}_k\}_{\text{force}}\{\boldsymbol{v}_k\}_{\text{force}}^T\right]$ – cf. Eq. (15) and (11), (12).

5.1. Collocated force

First a situation is considered where the force location is known exactly, hence: $\{\boldsymbol{w}_k\}_{\text{force}} = \{\boldsymbol{v}_k\}_{\text{force}} = 0$, and consequently $\mathbf{Q}_{\text{e}} = \mathbf{R}_{\text{e}} = \mathbf{S}_{\text{e}} = \mathbf{0}$. All modal states and forces are identified with high accuracy, allowing for an error-free extrapolation of the response by means of Eq. (10). Results are omitted due to space limitations.

5.2. Nodal force at 3L/4

For the next analysis, an equivalent force at $3L/4$ is used. In this case $\{\boldsymbol{w}_k\}_{\text{force}}$ and $\{\boldsymbol{v}_k\}_{\text{force}} \neq 0$, and consequently all error matrices ($\mathbf{Q}_{\text{e}}$, $\mathbf{R}_{\text{e}}$, $\mathbf{S}_{\text{e}}$) will become populated. Fig. 1a shows that the first modal displacement is identified relatively accurately. However, the discrepancies between simulated and estimated modal states become larger for the higher modes. To quantify these errors per state, an RMS error measure for each (normalised) modal state is defined in Eq.(17), where i is the mode number. Table 1 presents these RMS values for the current problem, clearly showing an increased error for the higher-order modes, with a maximum occurring in mode 4.

Fig. 1a and Table 1 show that the modal states and forces cannot be reconstructed uniquely, an effect caused by a violation of various assumptions used in the derivation of the estimator. Since the identified modal state estimates are incorrect, all data extrapolated on the basis of these estimates – see Eq. (10) and Fig. 1b – will also be incorrect.

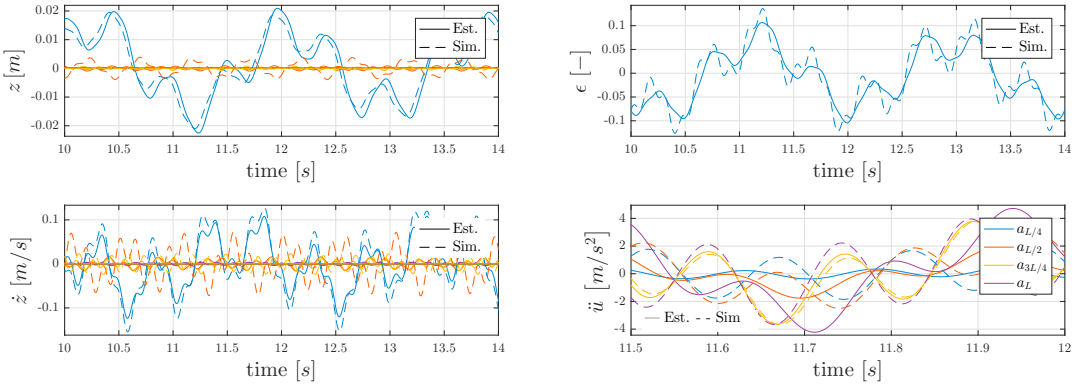

Fig. 1: Nodal equivalent force at $^{3L}/4$: True (solid lines) and estimated (dashed lines) time histories of (a) the modal states and (b) the predicted strain and accelerations.

The matrices $\mathbf{Q}_{\text{e},\mathbf{zz}}$ and $\mathbf{S}_{\text{e},\mathbf{zd}}$ are plotted in Fig. 2a and 2b. It is clear from the nonzero off-diagonal elements that the force error correlates the state errors, especially between modal displacements 2, 3, 4, 5 and 10. The effect hereof is clearly visible in the results presented in Table 1, where the largest relative error was found in modal state 4, corresponding to the location of the largest entry on the diagonal of $\mathbf{Q}_{\text{e},\mathbf{zz}}$ in Fig. 2a. Due to these unaccounted-for correlations, the algorithm is not able to uniquely identify the states.

Similar conclusions can be drawn considering the matrix $\mathbf{S}_{\text{e},\mathbf{zd}}$ in Fig. 2b: the force error strongly correlates the state error on modal displacement 4 with the measurement error on the tip acceleration, implying that it will be difficult to

Table 1: Nodal force at 3L/4: RMS values of normalised state estimate errors.

State, i:	1	2	3	4	5
$RMS_{z,i}$	8.63e-02	6.65e-01	6.00e-01	9.53e-01	6.92e-01
State, i:	6	7	8	9	10
$RMS_{z,i}$	3.19e-01	2.80e-01	2.38e-01	2.96e-01	7.26e-01

$$\mathrm{RMS}_{\mathbf{z},i} = \sqrt{\frac{1}{N}\sum_{k=1}^{N}\left(\frac{\mathbf{z}_k^i - \hat{\mathbf{z}}_k^i}{\max|\mathbf{z}^i|}\right)^2} \tag{17}$$

distinguish between (and thus uniquely identify) the force and modal state 4 on the basis of this measurement. Finally it is noted that the force error $\{\boldsymbol{w}_k\}_{\text{force}}$ in mode 4 corresponds to only 1.4% of the maximum value of modal state 4.

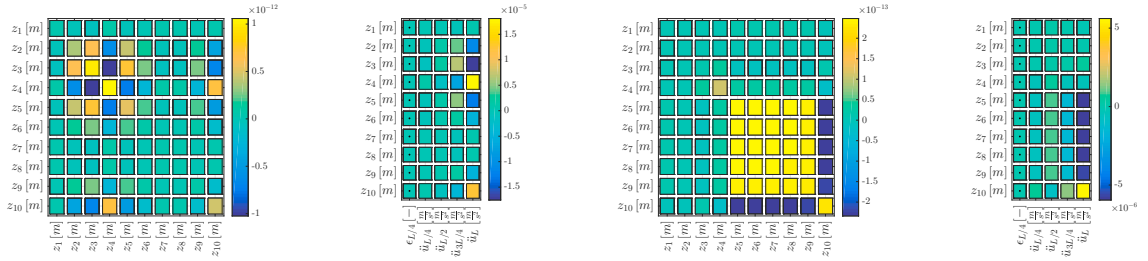

(a) (b) (c) (d)

Fig. 2: Error covariance matrices - Nodal equivalent force at $^{3L}/4$: (a) $\mathbf{Q}_{\mathrm{e},\mathbf{zz}}$ and (b) $\mathbf{S}_{\mathrm{e},\mathbf{zd}}$; Modal equivalent forces: (c) $\mathbf{Q}_{\mathrm{e},\mathbf{zz}}$ and (d) $\mathbf{S}_{\mathrm{e},\mathbf{zd}}$

5.3. Modal forces

A simple way to ensure that the states can be related to the forces in a unique way, is by the identification of modal equivalent forces [1]. Choosing the modal forces is crucial for an accurate response prediction, since the chosen modes must be able to represent the (dynamic and static) response of the structure. Two conflicting requirements arise in this regard: (1) a sufficient number of modal forces is required in order to assure an accurate response prediction over a possibly broad range of frequencies, (2) the number of equivalent modal forces is restricted by the number of acceleration and strain/displacement measurements through the direct invertibility criterion [11]. For the results presented in Fig. 3 and Table 2, four modal forces were identified in order to drive the modal response of the first four modes. For a system consisting of n_{m} modes and n_{p} modal forces, this is achieved by defining $\boldsymbol{\Phi}^{\mathrm{T}}\mathbf{S}_{\mathrm{p}} = \left[\mathbf{I}_{n_{\mathrm{p}}\times n_{\mathrm{p}}}\ \mathbf{0}_{n_{\mathrm{p}}\times(n_{\mathrm{m}}-n_{\mathrm{p}})}\right]^{\mathrm{T}}$ and then proceeding to construct $\mathbf{B}_{\mathrm{c}}$, $\mathbf{J}_{\mathrm{c}}$, $\mathbf{B}$ and $\mathbf{J}$ as in equations (4) and (7).

Table 2: Modal equivalent forces: RMS values of normalised state estimate error.

State, i:	1	2	3	4	5	6	7	8	9	10
$RMS_{z,i}$	5.27e-02	3.29e-02	6.77e-02	2.79e-01	4.99e-01	5.00e-01	5.00e-01	5.00e-01	5.00e-01	5.00e-01

As expected, the modal states and velocities are identified more accurately than in the previous case, allowing for an almost perfect reconstruction of the measured data – see Fig. 3b. The RMS state errors for some of the dominant modes in the response – especially mode 2 and 3 – are also significantly smaller than with nodal equivalent forces (cf. Table 1 and 2). It is interesting to note, though, that some spurious high-frequency components are present in the first identified modal displacement at the top left of Fig. 3a. These can be attributed to the existence of marginally stable zeros in the system. To satisfy the stability criteria [11], 3 additional strain sensors should be added to the measurement system in order to compensate for the 3 additional forces that are to be identified. From the results it appears that the unaccounted-for errors on states 5 to 10 – which result from the use of a reduced set of modal forces – are manifested in the form of an amplitude modulation of the 1st modal displacement in Fig. 3a, where it might have a significant influence on the accuracy of any strain or fatigue damage predictions at locations other than those measured.

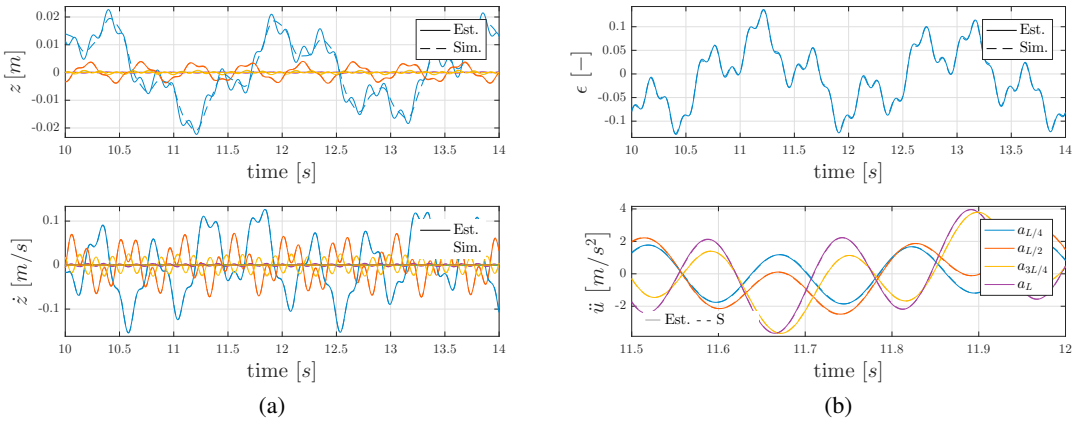

Fig. 3: Modal equivalent forces: True (solid lines) and estimated (dashed lines) time histories of (a) the modal states and (b) the predicted strain and accelerations.

6. Conclusions

Modal state and force estimates obtained with Kalman-type filters can be used to estimate the full-field response of a structure on the basis of limited sensor data. In this contribution, the focus was on situations where no knowledge on the applied loading is available, neither in terms of its dynamic content, nor its spatial distribution. In these situations response-driving equivalent forces are often identified, where it is generally assumed that an accurate response prediction can be achieved by simply ensuring that these equivalent forces meet the controllability requirements. It has been shown, however, that controllability is an insufficient condition for ensuring the accuracy of the full-field response estimates, and that they remain, in fact, very sensitive to a correct assumption on the force locations. This is mainly due to a violation of various assumptions regarding the correlation between the assumed noise processes, which directly influences the uniqueness of the estimated states and forces. The identification of modal equivalent forces can solve this problem, but will in many cases require an increase in the number of required sensors. Future work will include the development of a criterion for assessing the uniqueness of coupled input-state estimates, specifically, as well as an extension of the presented results to other commonly encountered engineering problems, e.g. that of moving loads.

References

[1] K. Maes, A. Iliopoulos, W. Weijtjens, C. Devriendt, G. Lombaert, Dynamic strain estimation for fatigue assessment of an offshore monopile wind turbine using filtering and modal expansion algorithms, Mechanical Systems and Signal Processing 76 (2016) 592–611.

[2] P. Van der Male, E. Lourens, Operational vibration-based response estimation for offshore wind lattice structures, in: Structural Health Monitoring and Damage Detection, Volume 7, Springer, 2015, pp. 83–96.

[3] T. Nord, E. Lourens, M. Määttänen, O. Øiseth, K. Høyland, Laboratory experiments to study ice-induced vibrations of scaled model structures during their interaction with level ice at different ice velocities, in: Cold Regions Science and Technology, 119, 2015, pp. 1–15.

[4] T. Nord, O. Øiseth, E. Lourens, Ice force identification on the nordstroemsgrund lighthouse, in: Computers and Structures, 169, 2016, pp. 24–39.

[5] C. Papadimitriou, C.-P. Fritzen, P. Kraemer, E. Ntotsios, Fatigue predictions in entire body of metallic structures from a limited number of vibration sensors using kalman filtering, in: Structural Control and Health Monitoring, 18(5), 2011, pp. 554–573.

[6] E. Lourens, C. Papadimitriou, S. Gillijns, E. Reynders, G. De Roeck, G. Lombaert, Joint input-response estimation for structural systems based on reduced-order models and vibration data from a limited number of sensors, Mechanical Systems and Signal Processing 29 (2012) 310–327.

[7] S. E. Azam, E. Chatzi, C. Papadimitriou, A. Smyth, Experimental validation of the Kalman-type filters for online and real-time state and input estimation, Journal of Vibration and Control (2015) 1077546315617672.

[8] S. Gillijns, B. De Moor, Unbiased minimum-variance input and state estimation for linear discrete-time systems with direct feedthrough 43 (2007) 934–937.

[9] D. Bernal, A. Ussia, Sequential deconvolution input reconstruction, Mechanical Systems and Signal Processing 50 (2015) 41–55.

[10] D. Bernal, Non-recursive sequential input deconvolution, Mechanical Systems and Signal Processing 82 (2017) 296–306.

[11] K. Maes, E. Lourens, K. Van Nimmen, E. Reynders, G. De Roeck, G. Lombaert, Design of sensor networks for instantaneous inversion of modally reduced order models in structural dynamics, Mechanical Systems and Signal Processing 52 (2015) 628–644.